SHEAR INSTABILITY IN SKIN TISSUE

Pasquale CIARLETTA, Michel DESTRADE, Artur L. GOWER

2013

Abstract

We propose two toy-models to describe, predict, and interpret the wrinkles appearing on the surface of skin when it is sheared. With the first model, we account for the lines of greatest tension present in human skin by subjecting a layer of soft tissue to a pre-stretch, and for the epidermis by endowing one of the layer's faces with a surface tension. For the second model, we consider an anisotropic model for the skin, to reflect the presence of stiff collagen fibres in a softer elastic matrix. In both cases, we find an explicit bifurcation criterion, linking geometrical and material parameters to a critical shear deformation accompanied by small static wrinkles, with decaying amplitudes normal to the free surface of skin.

1 Introduction

When the skin is pinched, wrinkles appear quite early on its surface. The same phenomenon occurs when the skin is sheared, i.e. pinched with one finger moving in one direction and the other fixed or moving in the opposite direction. In fact, pinching is one of the tests performed by dermatologists and surgeons [1] when trying to assess the direction of greatest tension [2] in the neighborhood of a site of interest. Sometimes called *lines of cleavage* [3], the orientations of the lines of greatest tension are crucial to the way a scar heals. For a cut across the lines, the lips of a wound will be pulled away from one another during the healing process, while they will be drawn together if the cut has occurred parallel to the lines. In one case the resulting scar can be quite unsightly, in the other it is almost invisible. In this paper we investigate the mechanical stability of two toy models for the human skin under shear in its plane, and view the onset of small-amplitude, unstable solutions as a prototype for skin wrinkling.

Of course, skin is a complex, multi-faced organ, and it is not easily, nor perhaps realistically, modeled. In Section 2, we first view it as an initially isotropic, neo-Hookean layer

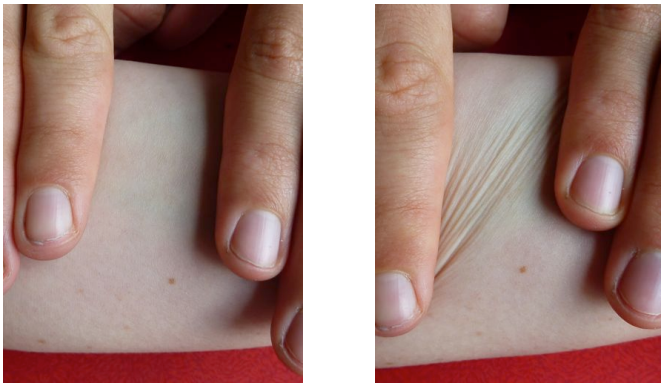

Figure 1: Shearing the forearm skin across the lines of cleavage (which run along the length of the arm) results in early onset of small-amplitude wrinkles.

of finite thickness. Although a two-layered model of skin would be more realistic, it would greatly complicate the theoretical analysis of the shear instability properties. Therefore, we prefer to consider an epidermis of vanishing thickness on top of a hyperelastic dermis, by defining a proper surface elastic energy. In other words we let one of the layer's faces be a material curve endowed with intrinsic elastic properties associated with extensibility, but no bending stiffness (see [4] for a rigorous exposition of such elastic coatings). We account for the lines of greatest tension by imposing a finite plane pre-stretch in a given direction; in other words, we simulate those lines through *strain-induced anisotropy*. Then we investigate whether surface energy and pre-stretch promote or attenuate the appearance of wrinkles when the layer is subject to simple shear in the direction of the cleavage lines.

In Section 3, we then view skin as being intrinsically *anisotropic* that is, we switch to the point of view that lines of greatest tension are due to the presence of families of parallel bundles of stiff collagen fibres imbedded in a softer elastin matrix. The introduction of even the simplest anisotropy – transverse isotropy due to a single privileged direction – complicates the equations of incremental instability greatly, and we thus restrict attention to a homogeneous solid without surface tension. We also omit finite-size effects by considering a half-space instead of a layer, and thus by focusing on the Biot surface instability phenomenon [5]. Here, the anisotropic contribution to the stored energy is that recently proposed by Ciarletta et al.[6]. Its polyconvexity ensures good properties from the physical point of view, such as strong ellipticity in compression, in contrast to the standard reinforcing model used recently by Destrade et al.[7] for the same stability study.

2 Shear instability for a neo-Hookean layer with surface coating

First we consider an isotropic elastic material of finite thickness H, undergoing an homogeneous shear. In order to mimic the response of human skin, we incorporate the presence of a residual stretch λ_{res} along the main cleavage lines, so that the base deformation field reads

$$x = \lambda_{\text{res}} X + (K/\lambda_{\text{res}})Y, \qquad y = Y/\lambda_{\text{res}}, \qquad z = Z, \tag{1}$$

where $\mathbf{x}$ is the current position of a material point which was at $\mathbf{X}$ in the reference configuration, and K is a constant. Hence, we see that the deformation can be decomposed as a plane stretch of amount λ_{res} followed by a simple shear of amount K, with deformation gradient $\mathbf{F}$ written as

$$\mathbf{F} = \begin{bmatrix} \lambda_{\text{res}} & K/\lambda_{\text{res}} & 0 \\ 0 & 1/\lambda_{\text{res}} & 0 \\ 0 & 0 & 1 \end{bmatrix} = \begin{bmatrix} 1 & K & 0 \\ 0 & 1 & 0 \\ 0 & 0 & 1 \end{bmatrix} \begin{bmatrix} \lambda_{\text{res}} & 0 & 0 \\ 0 & 1/\lambda_{\text{res}} & 0 \\ 0 & 0 & 1 \end{bmatrix}. \tag{2}$$

We note that the layer's thickness H remains unchanged through the deformation. For simplicity, we take the layer to be made of an isotropic neo-Hookean incompressible material with a surface energy at the free boundary $z = 0$, so that its total strain energy W reads

$$W = \frac{\mu}{2} \iiint (\text{tr } \mathbf{b} - 3)\, \mathrm{d}X\, \mathrm{d}Y\, \mathrm{d}Z + \iint \left(\gamma |\mathbf{x}_{,X} \times \mathbf{x}_{,Y}| + \frac{\mu_s}{2} (|\mathbf{x}_{,X}|^2 + |\mathbf{x}_{,Y}|^2 - 2) \right) \mathrm{d}X\, \mathrm{d}Y, \tag{3}$$

where μ is the shear modulus, $\mathbf{b} = \mathbf{F}\mathbf{F}^T$ is the left Cauchy-Green deformation tensor, γ is the surface tension coefficient, μ_s is the elastic shear modulus per surface unit, and the comma denotes partial derivative. This is akin to endowing one of the material boundary of the layer with a surface energy with a term proportional to changes in area (as is often done in fluid mechanics, see e.g. [8]), and another contribution depending on the elastic deformation of the surface. This last term is proportional to a stretch measure of the surface deformation tensor, which is chosen for invariance requirements because we consider this elastic layer as a hemitropic film [9].

Now from the constitutive assumptions in Eq.(3), we find that $\boldsymbol{\sigma}$, the Cauchy stress tensor corresponding to the large deformation in Eq.(1) is given by

$$\boldsymbol{\sigma} = \mu \mathbf{b} - p\mathbf{I}, \tag{4}$$

where p is a Lagrange multiplier due to the constraint of incompressibility. Writing that the boundary at $z = 0$ is traction-free fixes the value of p as $p = \mu$.

Straightforward calculations reveal that principal stretches of the deformation field in Eq.(1) are λ_k $(k = 1, 2, 3)$ given by [10]

$$\lambda_1 \pm \lambda_2 = \sqrt{(\lambda_{\rm res} \pm \lambda_{\rm res}^{-1})^2 + K^2 \lambda_{\rm res}^{-2}}, \qquad \lambda_3 = 1, \tag{5}$$

and that the Eulerian principal axes (x_1, x_2) are obtained after an anti-clockwise rotation of angle ϕ of the in-plane coordinate axes about the z axis, where

$$\tan(2\phi) = \frac{2K}{\lambda_{\rm res}^2 - \lambda_{\rm res}^{-2}(1 - K^2)}. \tag{6}$$

From Eq.(5), we note that

$$\lambda_2 = \lambda_1^{-1}, \qquad K = \lambda_{\rm res}\sqrt{(\lambda_1 - \lambda_1^{-1})^2 - (\lambda_{\rm res} - \lambda_{\rm res}^{-1})^2}. \tag{7}$$

We now look for a perturbation solution in the neighbourhood of the large deformation (1), using the theory of incremental deformations [11]. Hence we call $\mathbf{u} = \mathbf{u}(x_1, x_2, x_3)$ the incremental displacement field, for which the incremental incompressibility condition imposes that

$$u_{i,i} = 0. \tag{8}$$

The constitutive equation for the components of the incremental nominal stress $\dot{\mathbf{S}}$ reads in general as [11],

$$\dot{S}_{ji} = L_{jikl}\, u_{k,l} + p\, u_{j,i} - \dot{p}\, \delta_{ji}, \tag{9}$$

where $\dot{p}$ is the increment in the Lagrange multiplier, and L is the fourth-order tensor of instantaneous moduli, i.e. the push-forward of the fixed reference elasticity tensor. In the absence of body forces, we can therefore write the equilibrium equation of the incremental nominal stress $\dot{\mathbf{S}}$ as

$$(\mathrm{div}\, \dot{\mathbf{S}})_i = \dot{S}_{ji,j} = 0. \tag{10}$$

In the case of a neo-Hookean material, it is easy to check that the components of L are simply $L_{jikl} = \mu \delta_{jk} b_{il}$ so that Eq.(10) in the coordinate system aligned with the Eulerian principal axes takes the following simplified form

$$-\dot{p}_{,1} + \mu\lambda_1^2 u_{1,ii} = 0, \qquad -\dot{p}_{,2} + \mu\lambda_2^2 u_{2,ii} = 0, \qquad -\dot{p}_{,3} + \mu\lambda_3^2 u_{3,ii} = 0, \tag{11}$$

Differentiating these incremental equilibrium equations with respect to x_1, x_2, and x_3, respectively, and using the incremental incompressibility condition in Eq.(8), we find that

$$\nabla^2 \dot{p} = 0, \tag{12}$$

that is, the incremental Lagrange multiplier is a Laplacian field [12].

Now, for the incremental *boundary conditions*, we consider that the bottom $z = x_3 = -H$ of the layer is fixed (clamped condition):

$$u_i(x_1, x_2, -H) = 0, \tag{13}$$

while the top face $z = x_3 = 0$ remains free of incremental traction:

$$\begin{aligned} &u_{1,3} + u_{3,1} - \mu_s\lambda_1^2 u_{1,11} - \mu_s\lambda_1^{-2} u_{1,22} = 0, \\ &u_{2,3} + u_{3,2} - \mu_s\lambda_1^2 u_{2,11} - \mu_s\lambda_1^{-2} u_{2,22} = 0, \\ &-\dot{p} + 2\mu u_{3,3} - \gamma\left(u_{3,11} + u_{3,22}\right) - \mu_s\lambda_1^2 u_{3,11} - \mu_s\lambda_1^{-2} u_{3,22} = 0. \end{aligned} \tag{14}$$

We search for solutions to Eqs.(8,11,12) in the following form:

$$\{u_1, u_2, u_3, \dot{p}\} = \{U_1(x_3), U_2(x_3), U_3(x_3), ikP(x_3)\}\, e^{ik(\cos\theta\, x_1 + \sin\theta\, x_2)}, \tag{15}$$

corresponding to the occurrence of plane wrinkles with wavenumber k, forming an angle θ with the direction of maximum extension. It is easy to show that a solution in the form of Eq.(15) is given by [12]

$$\begin{aligned} U_1(x_3) &= \cos\theta \left(a_1 e^{-kx_3} + a_2 e^{-qkx_3} + a_3 e^{kx_3} + a_4 e^{qkx_3}\right), \\ U_2(x_3) &= \sin\theta \left(a_1 e^{-kx_3} + a_2 e^{-qkx_3} + a_3 e^{kx_3} + a_4 e^{qkx_3}\right), \\ U_3(x_3) &= i\left(a_1 e^{-kx_3} + a_2 e^{-qkx_3}/q - a_3 e^{kx_3} - a_4 e^{qkx_3}/q\right), \\ P(x_3) &= -\mu(1-q^2)\left(a_1 e^{-kx_3} + a_3 e^{kx_3}\right), \end{aligned} \tag{16}$$

where a_1, a_2, a_3, a_4 are yet arbitrary constants, and q is fixed by imposing Eqs.(11), as

$$q = \sqrt{\lambda_1^2 \cos^2\theta + \lambda_1^{-2}\sin^2\theta}. \tag{17}$$

Using Eqs.(16), it can be checked that only four independent boundary conditions result from Eqs.(14). Setting $\mathbf{a} = [a_1, a_2, a_3, a_4]^T$, they can be written in the following matrix form:

$$\mathbf{Q}\mathbf{a} = \mathbf{0}, \tag{18}$$

where the components of the matrix $\mathbf{Q}$ are

$$\begin{bmatrix} 2q - kq^2 L_{\mathrm{el}} & 1 + q^2 - kq^2 L_{\mathrm{el}} & -2q - kq^2 L_{\mathrm{el}} & -1 - q^2 - kq^2 L_{\mathrm{el}} \\ q(-1 - q^2 + kL_{\mathrm{cap}} + kq^2 L_{\mathrm{el}}) & -2q + kL_{\mathrm{cap}} + kq^2 L_{\mathrm{el}} & q(-1 - q^2 - kL_{\mathrm{cap}} - kq^2 L_{\mathrm{el}}) & -2q - kL_{\mathrm{cap}} - kq^2 L_{\mathrm{el}} \\ e^{kH} & e^{qkH} & e^{-kH} & e^{-qkH} \\ e^{kH} & e^{qkH}/q & -e^{-kH} & -e^{-qkH}/q \end{bmatrix}. \tag{19}$$

Here $L_{\rm cap} := \gamma/\mu$, $L_{\rm el} := \mu_s/\mu$ are the *characteristic capillary **and elastic** lengths* of the material, respectively. The resulting condition for the wrinkling instability is $\det \mathbf{Q} = 0$. After lengthy manipulations not reproduced here, it is possible to show that the earliest onset of instability occurs at $\theta = 0$ that is, when the wrinkles are aligned with the direction where the greatest stretch, λ_2, takes place. There, $q = \lambda_1$, and the *dispersion relation* reduces to

$$\begin{aligned} k\lambda_1^2 L_{\rm el} \big\{ \big[2kL_{\rm el}\lambda_1^3 - (\lambda_1^2-1)^2 \sinh(\lambda_1 kH)\big] \cosh(kH) \\ -kL_{\rm el}\lambda_1^2 \big[2\lambda_1 + (1+\lambda_1^2)\sinh(\lambda_1 kH)\sinh(kH)\big]\big\} \\ + k^2\lambda_1^2 L_{\rm el}L_{\rm cap}\big[-2\lambda_1 + 2\lambda_1\cosh(kH)\cosh(\lambda_1 kH) - (1+\lambda_1^2)\sinh(kH)\sinh(\lambda_1 kH)\big] \\ + kL_{\rm cap}(\lambda_1^2-1)\left[\cosh(kH)\sinh(\lambda_1 kH) - \lambda_1\sinh(kH)\cosh(\lambda_1 kH)\right] \\ + 4\lambda_1(\lambda_1^2+1) - \lambda_1(5+2\lambda_1^2+\lambda_1^4)\cosh(kH)\cosh(\lambda_1 kH) \\ + (1+6\lambda_1^2+\lambda_1^4)\sinh(kH)\sinh(\lambda_1 kH) = 0. \end{aligned} \quad (20)$$

This dispersive bifurcation criterion is the main result of this section, linking the material ($L_{\rm cap}$, $L_{\rm el}$) and geometrical ($\lambda_{\rm res}$ and K appearing inside the expression for λ_1 in Eq.(5)) parameters describing the sheared layer, to the wavelength of the expected wrinkles (through the non-dimensional quantity $kH = 2\pi H/\ell$, where ℓ is the wrinkles' wavelength).

Figure 2: Anecdotal evidence suggests that shearing the forearm skin along the lines of cleavage (which run along the length of the arm) results in later onset of small-amplitude wrinkles than when shearing across, compare with Figure 1.

In Figure 3 we show the separate influences of the pre-stretch and of the surface energy. We plot the critical amount of shear K^*, at which wrinkles occur, against H/ℓ, the ratio of the layer's thickness to the wrinkles' wavelength. We find that as H/ℓ becomes small,

K^* increases rapidly, showing that the layer is more and more stable: that is because for a thin slab, the clamped boundary condition at the bottom takes precedence and prevents the apparition of wrinkles. As soon as the layer's thickness becomes comparable to the wrinkles' wavelength ($H/\ell > 1$), the value of the critical amount of shear tends rapidly to its value for a semi-infinite solid (surface instability). On Figure 3 (left), we study the influence of $\lambda_{\rm res}$ in the absence of surface energy ($L_{\rm cap} = L_{\rm el} = 0$). We see that K^* is increased when $\lambda_{\rm res} > 1$ and decreased when $\lambda_{\rm res} < 1$. In other words, shearing along the direction of tension requires a greater amount of shear than shearing along the direction of compression, consistent with experimental observations, see Figure 2. On Figure 3 (right), we investigate the influence of surface tension ($L_{\rm cap} > 0, L_{\rm el} = 0$) in the absence of pre-stretch ($\lambda_{\rm res} = 1$). We see that as $L_{\rm cap}$ increases, K^* also increases, indicating that surface tension makes the layer more stable. A similar type of behaviour is obtained setting $L_{\rm cap} = 0, L_{\rm el} > 0$, but it is not shown here for the sake of brevity. This observation is consistent with the observation that young skin does not wrinkle as early as older skin when sheared, because it is tauter.

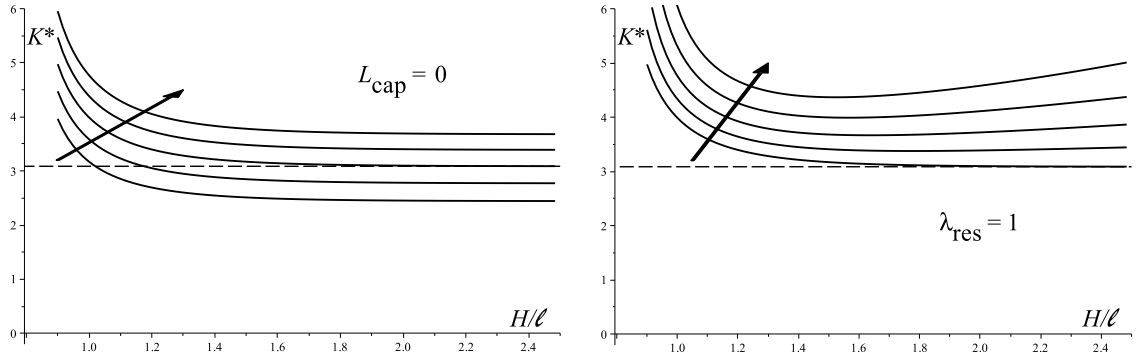

Figure 3: Left: In the absence of surface tension ($L_{\rm cap} = 0$), the layer becomes more (less) stable when sheared in the direction of tension (compression). Here $\lambda_{\rm res} = 0.8, 0.9, 1.0, 1.1, 1.2$. Right: In the absence of pre-stretch ($\lambda_{\rm res} = 1$), the layer becomes more stable in shear when its top surface is endowed with a surface tension. Here $L_{\rm cap}/H = 0.0, 0.005, 0.01, 0.015, 0.02, 0.025$, $L_{\rm el} = 0$. The horizontal line indicates the shear threshold of surface instability $K^* = 3.0873$ in an unstretched half-space without surface tension.

Owing to the rapid settling of the dispersion curves to their half-space (Biot) instability limit, we now take $kH \gg 1$ in Eq.(20), while keeping $kL_{\rm cap} = 2\pi L_{\rm cap}/\ell$, $kL_{\rm el} = 2\pi L_{\rm el}/\ell$

finite. It then reduces to

$$2\pi(L_{\rm el}/\ell)\lambda_1^2\left\{\lambda_1\left[1+2\lambda_1+\lambda_1^2+2\lambda_1^2\pi(L_{\rm el}/\ell)\right]-\frac{\lambda_1-1}{\lambda_1+1}2\pi(L_{\rm cap}/\ell)\right\}$$
$$+2\pi(L_{\rm cap}/\ell)(\lambda_1+1)+(\lambda_1^3+\lambda_1^2+3\lambda_1-1)=0. \quad (21)$$

To check for consistency, we make the link with known results. For instance, when we neglect the surface energy in Eq.(21) by taking $L_{\rm el}=L_{\rm cap}=0$, we recover the surface instability criterion of plane strain [7],

$$\lambda_2=\lambda_1^{-1}=\frac{3(13+3\sqrt{33})^{1/3}}{2^{1/3}(13+3\sqrt{33})^{2/3}-2^{8/3}-(13+3\sqrt{33})^{1/3}}\simeq 3.3830. \quad (22)$$

The corresponding *shear threshold* K^* is found by using Eq.(7), as

$$K^*=\lambda_{\rm res}\sqrt{\frac{2^{11/3}3^{2/3}}{3(9+\sqrt{33})^{1/3}}+\frac{4(45+6\sqrt{33})^{1/3}}{3}-(\lambda_{\rm res}-\lambda_{\rm res}^{-1})^2}\simeq\lambda_{\rm res}\sqrt{(3.0873)^2-(\lambda_{\rm res}-\lambda_{\rm res}^{-1})^2}. \quad (23)$$

Here the value $K^*=3.0873$, obtained in the absence of a pre-stretch ($\lambda_{\rm res}=1$), corresponds to the shear threshold of surface instability for a neo-Hookean half-space as found both theoretically by Destrade et al.[7] and experimentally by Mora et al.[13]. Figure 4 confirms the trends found from the exact dispersion equation. Hence the left figure (based on Eq.(23)) shows that the shear threshold K^* is enhanced (half-space is more stable) by the presence of a tensile pre-stretch and vice-versa for a compressive pre-stretch (in tension, K^* eventually reaches a maximum of 5.68 at $\lambda_{\rm rs}\simeq 2.40$, but this is way beyond the elastic limit of skin). Similarly, the effect of surface tension is to increase the stretchability of the half-space before it becomes unstable, as shown by the right figure (based on Eq.(21)).

The effect of the surface energy is to fix the wavelength at threshold, as already discussed for the surface instability of compressed skin tissues [14]. If $L_{\rm cap}/H\ll 1$ and $L_{\rm el}=0$, in particular, a logarithmic correction can be calculated by series development of Eq.(20), reading:

$$K=K^*+\beta(\lambda_{\rm res})\frac{L_{\rm cap}}{H}\log\left[\alpha(\lambda_{\rm res})\frac{H}{L_{\rm cap}}\right],\qquad kH=\tfrac{1}{2}\log\left[\alpha(\lambda_{\rm res})\frac{H}{L_{\rm cap}}\right], \quad (24)$$

with $\alpha(\lambda_{\rm res})=\lambda_{\rm res}(-0.0289+0.0025(\lambda_{\rm res}+\lambda_{\rm res}^{-2})$, $\beta(\lambda_{\rm res})=0.388\lambda_{\rm res}\sqrt{9.351-(\lambda_{\rm res}+\lambda_{\rm res}^{-2})^2}$.

To summarise the results of this section, we have found that the presence of a surface energy always stabilizes the free surface and fixes the morphology of the sheared surface.

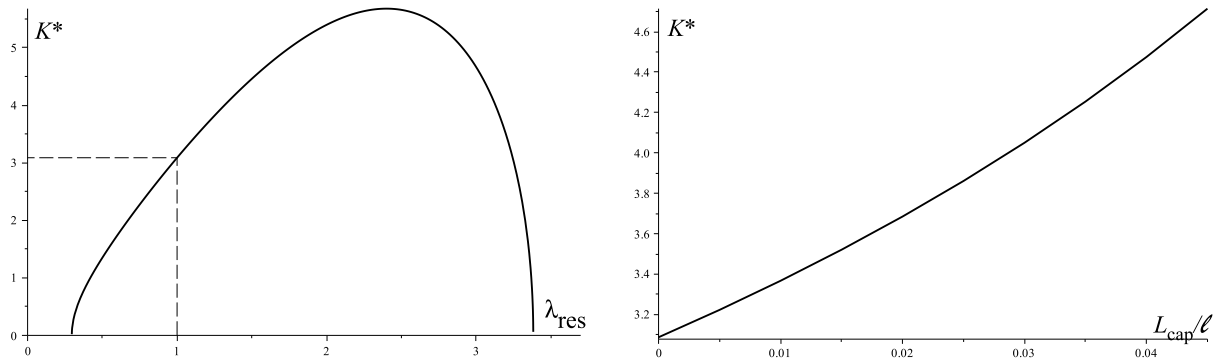

Figure 4: Stability of a semi-infinite neo-Hookean subject to a pre-stretch followed by a simple shear. Left: In the absence of surface tension $L_{\text{cap}} > 0$, the stability under shear is enhanced by a tensile pre-stretch ($\lambda_{\text{res}} > 1$ and decreased by a compressive pre-stretch ($\lambda_{\text{res}} < 1$). The dotted lines correspond to the shear threshold with no pre-stretch ($\lambda_{\text{res}} = 1$, $K^* = 3.0873$). Right: The presence of surface tension ($L_{\text{cap}} > 0$, $L_{\text{el}} = 0$) allows the half-space to be sheared further before the instability criterion is met ($K^* > 3.08$, the shear threshold in the absence of surface tension.)

3 Shear instability of a fibre-reinforced skin tissue

The dermis of human skin is characterized by a structural arrangement of elastin and collagen type I fibres in the extracellular matrix, leading to an anisotropic stiffening of the tissue. The aim of this section is to investigate how such a material anisotropy affects the stability properties of the sheared skin.

Let us consider a single family of fibre reinforcement oriented, in the reference configuration, along the unit vector $\mathbf{M} = [\cos\alpha, \sin\alpha, 0]^T$, defining the structural tensor $\widehat{\mathbf{M}} = \mathbf{M} \otimes \mathbf{M}$ so that $\lambda_\alpha := (\mathbf{C} : \widehat{\mathbf{M}})^{\frac{1}{2}}$ represents the fibre stretch, where $\mathbf{C}$ is the right Cauchy-Green deformation tensor. In order to build a strain measure for the fibres, we introduce the structural invariant I_α, defined as follows:

$$I_\alpha = \left[\mathbf{C} + \mathbf{C}^{-1} - 2\mathbf{I}\right] : \widehat{\mathbf{M}} = (\lambda_\alpha - \lambda_\alpha^{-1})^2 \tag{25}$$

As discussed in [6], this choice provides a physically consistent deformation measure when $\lambda_\alpha \to +\infty$ *and* when $\lambda_\alpha \to 0$, thereby allowing to account both for compression and extension of the fibres. Accordingly, the strain energy density of the skin tissue is defined as:

$$w = \frac{\mu}{2}(I_1 - 3) + \beta I_\alpha, \tag{26}$$

where $\beta > 0$ is the anisotropic elastic modulus for the fibre reinforcement. The constitutive relation Eq.(26) ensures strong-ellipticity of the tissue in planar deformations, a characteristic which is not met for example for the so-called standard model of fibre reinforcement chosen by [7]. It is a simple exercise to show that for a small tensile strain along the direction of the fibres, we have $\lambda_1 = \lambda_\alpha = 1 + \epsilon$, where $|\epsilon| \ll 1$ for the tensile stretch and $\lambda_2 = \lambda_3 = 1 - \epsilon/2$ for the lateral stretches; then, the resulting infinitesimal stress is $\sigma_1 = 4\mu\epsilon + 8\beta\epsilon$, showing that (at least in the linear regime) the ratio $2\beta/\mu$ is a measure of the stiffness of the fibres compared to the stiffness of the matrix.

We set $\lambda_{\rm res} = 1$ in this section for the sake of simplicity, so that the half-space is subject to *simple shear* only,

$$x = X + KY, \qquad y = Y, \qquad z = Z, \tag{27}$$

with deformation gradient and principal stretches

$$\mathbf{F} = \begin{bmatrix} 1 & K & 0 \\ 0 & 1 & 0 \\ 0 & 0 & 1 \end{bmatrix}, \qquad \lambda_{1,2} = \pm\frac{K}{2} + \sqrt{1 + \frac{K^2}{4}}, \qquad \lambda_3 = 1, \tag{28}$$

respectively. It is then easy to show that $I_\alpha = K^2$, so that the total strain energy does not depend on fibre orientation, only on the amount of shear K. The corresponding Cauchy stress tensor does depend on fibre orientation, as follows

$$\boldsymbol{\sigma} = \mu(\mathbf{b} - \mathbf{I}) + 2\beta(\mathbf{FM} \otimes \mathbf{FM} - \mathbf{F}^{-T}\mathbf{M} \otimes \mathbf{F}^{-T}\mathbf{M}). \tag{29}$$

Let us look for a perturbed surface wave in the form of Eq.(15); to do so we need the components of the instantaneous moduli tensor L in Eq.(9). For the anisotropic strain energy density w defined in Eq.(26) and $\mathbf{F}$ given in Eq.(28) we find the components

$$\begin{aligned} &L_{jikl} = \mu\delta_{jk}b_{il} + \\ &2\beta\left(M_pM_q\delta_{jk}F_{lp}F_{iq} + M_pM_q\delta_{jl}F^{-1}_{pk}F^{-1}_{qi} + M_pM_q\delta_{il}F^{-1}_{pk}F^{-1}_{qj} + M_pM_q\delta_{ik}F^{-1}_{pj}F^{-1}_{ql}\right), \end{aligned} \tag{30}$$

in the coordinate system aligned with the directions of simple shear x, y, z (see Appendix for explicit expressions). Then we take the incremental quantities to be of the form

$$\{u_j, \dot{S}_{3j}, \dot{p}\} = \{U_j(kz), ik\,S_{3j}(kz), ik\,P(kz)\}e^{ik(\cos\theta\,x + \sin\theta\,y)}, \tag{31}$$

where the amplitudes are functions of kz only. By a well established procedure we can use Eqs.(8-10) to eliminate P and write the incremental equations as a first-order differential system known as the *Stroh formulation*,

$$\boldsymbol{\eta}' = i\mathbf{N}\boldsymbol{\eta} = i\begin{bmatrix} \mathbf{N}_1 & \mathbf{N}_2 \\ \mathbf{N}_3 & \mathbf{N}_1^T \end{bmatrix}\boldsymbol{\eta}, \qquad \text{with} \quad \boldsymbol{\eta} := [U_1, U_2, U_3, S_{31}, S_{32}, S_{33}]^T, \tag{32}$$

where the prime denotes differentiation with respect to the function argument kz. Here it turns out that the blocks $\mathbf{N}_1$, $\mathbf{N}_2$ and $\mathbf{N}_3$ are symmetric (explicit expressions are given in the Appendix).

All is in place now for a complete resolution of the surface instability problem. There exist many strategies for this resolution, see a partial list and references in Destrade et al.[7]. Here we adopted a straightforward approach, because it turned to be tractable numerically. Noticing that the Stroh matrix $\mathbf{N}$ is constant, a solution of the system Eq.(32) has the form

$$\boldsymbol{\eta} = \boldsymbol{\eta}_0 e^{ikqz} \qquad \text{with} \qquad \boldsymbol{\eta}_0 := [\mathbf{U}_0, \mathbf{S}_0]^T, \tag{33}$$

where $\boldsymbol{\eta}_0$ is a constant vector and q are the eigenvalues of $\mathbf{N}$. In order for the wrinkles' amplitude to decay with depth, we retain the three roots q_1, q_2, q_3 with positive imaginary part (i.e. $\mathrm{Im}(q) > 0$). This gives the following general solution,

$$\boldsymbol{\eta}(kz) = c_1\boldsymbol{\eta}_1 e^{ikq_1 z} + c_2\boldsymbol{\eta}_2 e^{ikq_2 z} + c_3\boldsymbol{\eta}_3 e^{ikq_3 z} = \begin{bmatrix} \mathbf{A} \\ \mathbf{B} \end{bmatrix} \begin{bmatrix} c_1 \\ c_2 \\ c_3 \end{bmatrix}, \tag{34}$$

where c_1, c_2, c_3 are constants, and $\mathbf{A}$, $\mathbf{B}$ are square (3×3) matrices built from the eigenvectors $\boldsymbol{\eta}_i$ $(i = 1, 2, 3)$, taken proportional to any column vector of the matrix adjoint to $(\mathbf{N} - q_i\mathbf{I})$. Now, the traction-free boundary condition at $z = 0$ can be written as :

$$\mathbf{S}_0 = \begin{bmatrix} S_{31}(0) \\ S_{32}(0) \\ S_{33}(0) \end{bmatrix} = \mathbf{Z} \begin{bmatrix} U_1(0) \\ U_2(0) \\ U_3(0) \end{bmatrix} = \mathbf{Z}\mathbf{U}_0 = \mathbf{0}, \tag{35}$$

where $\mathbf{Z} := -i\mathbf{B}\mathbf{A}^{-1}$ is the surface impedance matrix. The condition for the onset of a surface instability is thus

$$\det \mathbf{Z} = 0. \tag{36}$$

As we do not know *a priori* in which directions the wrinkles are to appear for a given angle α of the fibres with respect to the direction of shear, we need to span the entire plane and find the angle θ^* for which the corresponding amount of shear K^* is minimal, indicating the earliest onset of wrinkling. This is the main difference of instability behaviour between an isotropic material (such as the material in the previous section), where the wrinkles appear *aligned* with a principal direction of pre-deformation, and an anisotropic material, where the wrinkles may be *oblique* with respect to the direction of least stretch.

For our simulations, we chose material constants such that $2\beta/\mu = 0$ (matrix alone), 0.4 (matrix stiffer than fibres), 1.0 (matrix as stiff as fibres), and 2.0 (matrix softer than

fibres). For each choice of $2\beta/\mu$ we found K^* and θ^* as functions of α. Varying the angle α can be interpreted as either varying orientation of the fibres for a shear that occurs along a fixed axis, such as the y-axis in Eq. (27), or as varying the axis along which shear is taking place for a fixed fibre direction α. For illustrative purposes, a typical surface buckling solution is depicted in Figure 6, where we chose $\beta/\mu = 1$ (fibres are twice stiffer than matrix in linear regime) and $\alpha = 84.5°$ (fibres are originally almost at right angle to the direction of shear): there, according to Figure 5, we have $K^* = 1.51$ and $\theta^* = 115.2°$.

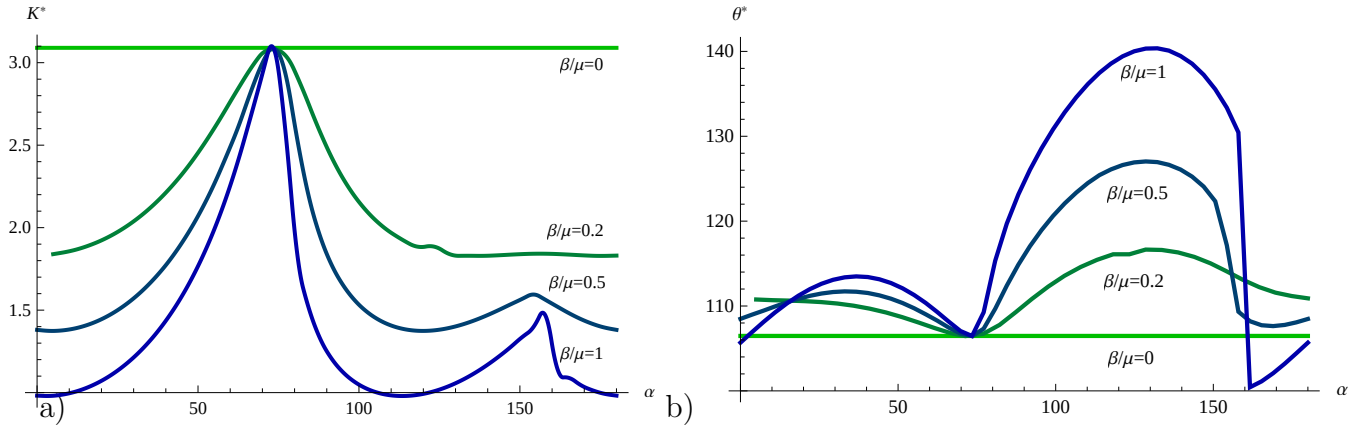

Figure 5: (a) The critical shear strain K^* as a function of the reference fibre angle α: The presence of fibres clearly leads to earlier surface instability in shear. (b) The critical instability angle θ^* as a function of the reference fibre angle α: These results are harder to interpret because θ^* is defined in the current configuration and α in the reference configuration. A remapping of the variations of K^* and θ^* with the current fibre angle is shown in Figure 8.

To set the stage for analyzing the results in Figure 5, we note that the first wrinkles to appear will occupy the least energy configuration possible while satisfying the zero traction boundary condition. When the half-space is sheared, line elements are compressed in certain directions and elongated in others. The effect of superposing a small-amplitude wrinkle is to alternatively elongate and compress the material along the direction of the wrinkle front, i.e. in the direction θ given by Eq. (31), see Figure 7(a). This alternating behaviour, along with the zero traction boundary condition, makes it difficult to informally comprehend the influence of the wrinkle orientation, however we do notice a pattern. In the neo-Hookean isotropic case ($\beta = 0$), the wavefront is along the direction of greatest compression: hence here, wrinkling the material in a direction under compression, due to the shear, allows the material to release some potential energy. In the anisotropic case

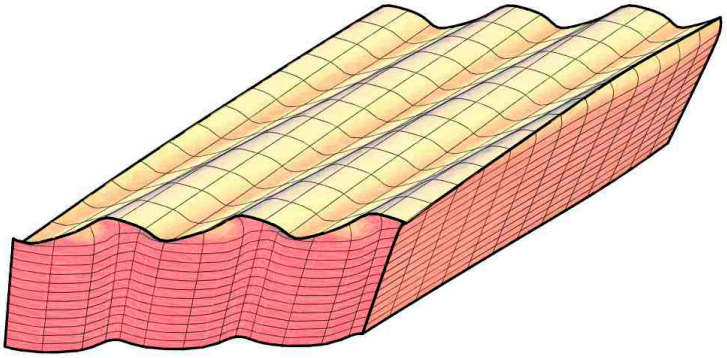

Figure 6: When $2\beta/\mu = 2.0$ (fibres are twice stiffer than matrix in linear regime) and $\alpha = 84.5°$ (fibres are almost at right angle to the direction of shear), the first wrinkles appear when the amount of shear reaches $K^* = 1.51$, and the corresponding angle of the wrinkles with respect to the direction of shear is $\theta^* = 115.2°$. Note the decay of the wrinkles' amplitude with depth.

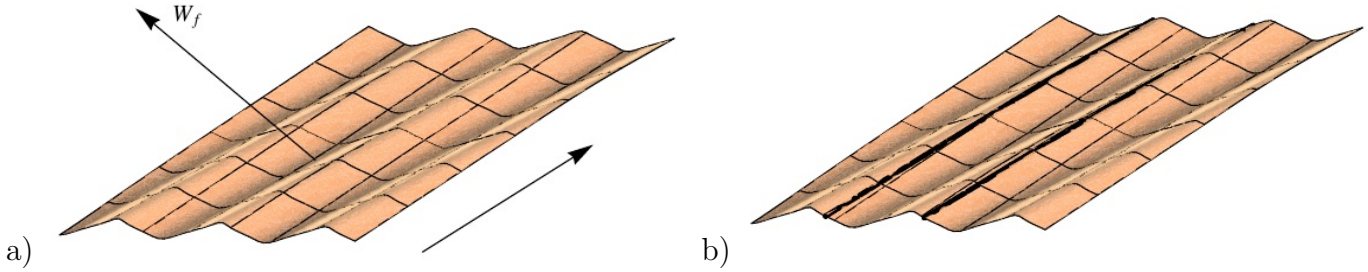

Figure 7: a) The wavefront of the wrinkle is indicated by the vector $\mathbf{W}_f$. Along the wavefront the material is alternatively elongated and compressed, orthogonal to it the material is neither elongated nor compressed. b) The fibres are shown by bold black lines.

($\beta \neq 0$), the presence of fibres makes the wavefront of the first wrinkle tend towards being orthogonal to the fibres. For instance, Figure 7(b) depicts the fibre orientation for the solution in the previous figures.

Clearly the *current* direction of fibres (in the deformed state of finite simple shear), is

closely linked to the value to the wavefront orientation θ^*. To study this relationship we re-examine the data in Figure 5 by mapping α to the fibre orientation in the deformed body α^*, that is the angle between the spatial vector **FM** of the current fibre orientation and the x-axis, from which θ^* is also measured. The results of this remapping are shown in Figure 8.

We first turn our attention to the plots of K^* against α^*, see Figure 8(a). On the dashed lines, the fibres are neither compressed or stretched. The (almost straight) continuous black lines S_α and C_α indicate when the fibres are aligned with the directions of greatest stretch and greatest compression, respectively. They are given by the equations

$$\alpha^* = \tan^{-1}(\lambda_2), \qquad \alpha^* = \tan^{-1}(\lambda_1), \tag{37}$$

respectively, where the λs are given in Eq.(28) and evaluated at $K = K^*$. The S_α curve helps us elucidate why there exists a point (denoted p_C) where all anisotropic materials become unstable in shear at the same threshold shear $K^* \simeq 3.0873$ as in an isotropic neo-Hookean material (where $\beta = 0$): clearly, this phenomenon occurs when the shear is such that the fibres are aligned with the direction of greatest stretch. Then, it turns out that great simplifications occur in the Stroh formulation of the instability problem, and that the buckling criterion coincides with that of the neo-Hookean model, see proof in the Appendix. This is an artifact of our specific choice of strain energy density in Eq.(26).

In Figure 8(b), displaying the plots of θ^* against α^*, we drew the line $\theta^* = \alpha^* - 90^\circ$. Clearly, in a region close to p_C, the wavefront is almost aligned with the fibres, as is the case in an isotropic neo-Hookean material. As β/μ increases, the neighborhood of this alignment widens, indicating that the stiffer the fibres are, the closer the instability curves in Figure 8(b) will be to the line $\theta^* = \alpha^* - 90^\circ$ and the less the wrinkles will alter the extended fibres.

The overall general conclusion is that stiffer fibres lead to earlier onset of instability (notwithstanding the punctual fixing of all curves at point p_C, due to the very special case where fibres end up being aligned with the direction of greatest stretch in the deformed configuration.) This result is in agreement with the casual observation that old skin (presumably with stiffer collagen bundles) wrinkles earlier than young skin when pinched.

4 Discussion and Conclusion

In this work we have investigated the occurrence of shear instability in skin tissue within the framework of nonlinear elastic theories.

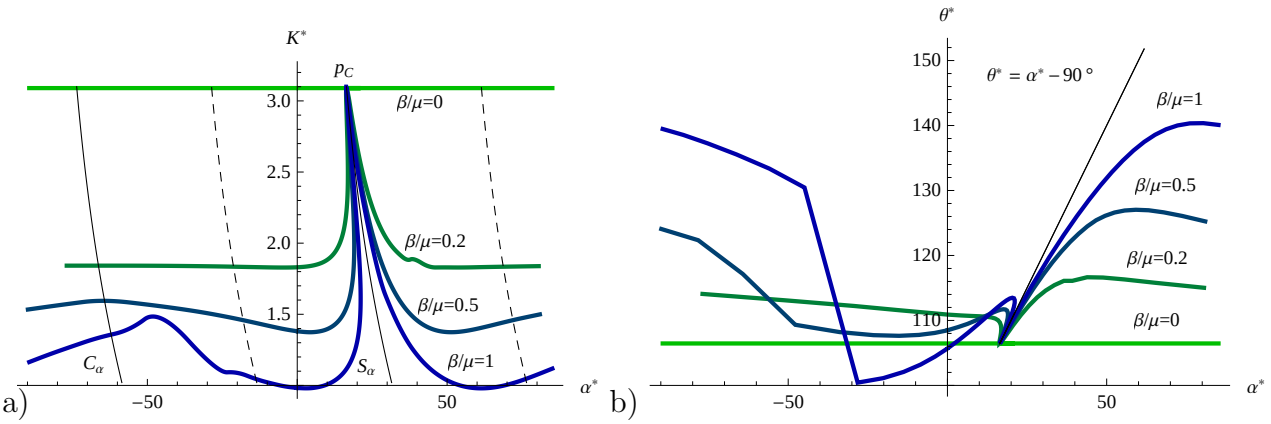

Figure 8: (a) The critical shear strain K^* as a function of the current angle the fibres α^* with respect to the direction of shear. (b) The critical instability angle θ^* as a function of α^*. The point p_C indicates a surface instability state common to all materials (independent of the material parameters).

In Section 2, we have considered the skin tissue as a neo-Hookean layer of finite thickness, whilst the epidermis is modeled *as a hemitropic film with given surface energy*. Moreover, we have taken into account the presence of the cleavage lines of skin as preferred direction of residual stretches inside the tissue. Under these assumptions, a linear stability analysis has been performed using the method of incremental elastic deformations, and an analytical form of the dispersion relation has been reported in Eq. (20). The results demonstrate that the presence of surface energy makes the layer more stable, in the sense that it needs to be sheared more for wrinkles to develop than when surface energy is absent (Figure 3(a)). Furthermore, the surface energy fixes the surface instability wavelength at threshold at a finite value, as depicted in Figure 3(b). We have also found that wrinkles appear earlier when the shear takes place perpendicular to the direction of pre-stretch than when it occurs along that direction, as confirmed by the anectodal evidences shown in Figures 1 and 2.

In Section 3, we have investigated the effect of fibre reinforcement in the dermis layer on the shear instability characteristics. For this purpose, we have used the polyconvex strain energy function in Eq.(26) for modeling the transverse isotropic reinforcement along a preferential fibre direction. A Stroh formulation of the incremental elastic equations has been derived in Eq. (32), and solved numerically using an iterative technique. As shown in Figures 5 and 8, we have found that the presence of fibres always lowers the shear threshold at which geometrical instability happens: the stiffer the fibres, the earlier the wrinkles appear in shear. Considering that anisotropic stiffness of skin greatly increase

with ageing [15], our results are in agreement with the fact that older skin wrinkles earlier when pinched.

The presence of a universal point of instability at shear threshold $K^* \simeq 3.09$ when the fibres are aligned with the direction of greatest stretch λ_2, irrespective of the value of β/μ, can be observed on Figures 5 and 8. This anchor point is present for $\alpha_{\rm cr} = \tan^{-1}(\lambda_2) \simeq 73.53^\circ$ no matter how stiff the fibres are compared to the matrix (In the Appendix we identify its origin.) However, it represents a very special case of shear, and when we move away from the region of influence of this point, we notice that all bifurcation curves indicate a significant lowering of the shear threshold of instability (as soon as the fibres become at least as stiff as the matrix, $\beta/\mu \leq 1$). In experimental tests (see e.g. Nì Annaidh et al.[16]), collagen fibres in human skin are determined to be at least 500 times stiffer than the elastin matrix. We may thus deduce that our model, away from the anchor point, predicts that surface instability will occur early, at low levels of shear, in line with the visual observations of Figures 1 and 2.

In conclusion, this mathematical study of wrinkle formation in sheared skin confirms that pinching experiments in dermatology are useful tools to evaluate the local mechanical properties of the tissue.

References

[1] J.C. Waldorf, G. Perdikis,and S.P. Terkonda, Planning incisions, *Oper. Tech. Gen. Surg.* **4** (2002) 199-206.

[2] C.J.Kraissl, The selection of appropriate lines for elective surgical incisions. *Plastic Reconstr. Surg.* **8** (1951) 1-28.

[3] H.T. Cox, The cleavage lines of the skin. *Br. J. Surg.* **29** (1941) 234-240.

[4] D.J. Steigmann, and R.W. Ogden, Plane deformations of elastic solids with intrinsic boundary elasticity, *Proc. Roy. Soc. Lond.* **A453** (1997) 853-877.

[5] M.A. Biot, Surface instability of rubber in compression. *Appl. Sci. Research* **A12** (1963) 168-182.

[6] P. Ciarletta, I. Izzo, S. Micera, and F. Tendick, Stiffening by fibre reinforcement in soft materials: A hyperelastic theory at large strains and its application, *J. Biomech. Behavior Biomed. Mat.* **4** (2011) 1359-1368.

[7] M. Destrade, M.D. Gilchrist, D.A. Prikazchikov, and G. Saccomandi, Surface instability of sheared soft tissues. *J. Biomech. Eng.* **130** (2008) 061007, 1-6.

[8] B. Lautrup, *Physics of Continuous Matter* (2nd Ed., CRC Press, Boca Raton 2011).

[9] D.J. Steigmann, and R.W. Ogden, Elastic surface-substrate interactions, *Proc. Roy. Soc. Lond.* **A455** (1999) 437-474.

[10] M. Destrade, and R.W. Ogden, Surface waves in a stretched and sheared incompressible elastic material, *Int. J. Non-Linear Mech.* **40** (2005) 241-253.

[11] R.W. Ogden, *Nonlinear Elastic Deformations* (Dover, New York 1997).

[12] J.N. Flavin, Surface waves in pre-stressed Mooney material, *Q. J. Mech. Appl. Math.* **16** (1963) 441-449.

[13] S. Mora, M. Abkarian, H. Tabuteau, and Y. Pomeau, Surface instability of soft solids under strain. *Soft Matter* **7** (2011) 10612-10619.

[14] P. Ciarletta, and M. Ben Amar, Papillary networks in the dermal-epidermal junction of skin: A biomechanical model. *Mech. Res. Comm.* **42** (2012) 68-76.

[15] P.G. Agache, C. Monneur, J.L. Leveque, and J. De Rigal, Mechanical properties and Young's modulus of human skin in vivo. *Arch. Dermatol. Res.* **269** (1980) 221-232.

[16] A. Ni Annaidh, K. Bruyere, M. Destrade, M.D. Gilchrist, C. Maurini, M. Ottenio, G. Saccomandi, Automated estimation of collagen fibre dispersion in the dermis and its contribution to the anisotropic behaviour of skin. Annals Biomed. Eng. **40** (2012) 1666-1678.

Appendix

For an incompressible anisotropic material with strain energy density w given in Eq.(26), there are 31 non-zero instantaneous moduli in the coordinate system aligned with the

directions of simple shear x, y, z in Eq.(27). They are found from Eq.(30) as follows.

$$
\begin{aligned}
&L_{1111} = \mu(1+K^2) + 2\beta(4\cos^2\alpha + 2K\cos\alpha\sin\alpha + K^2\sin^2\alpha),\\
&L_{1112} = L_{1211} = L_{2122} = L_{2221} = 4\beta\cos\alpha(\sin\alpha - K\cos\alpha),\\
&L_{1121} = L_{1222} = L_{2111} = L_{2212} = \mu K + 2\beta(\sin 2\alpha - K\cos 2\alpha),\\
&L_{1212} = (\mu+2\beta)(1+K^2),\\
&L_{1221} = L_{2112} = 2\beta(1 - 2K\cos\alpha\sin\alpha + K^2\cos^2\alpha),\\
&L_{1313} = \mu(1+K^2) + 2\beta(\cos\alpha + K\sin\alpha)^2,\\
&L_{1323} = L_{2313} = \mu K + 2\beta\sin\alpha(\cos\alpha + K\sin\alpha)^2,\\
&L_{1331} = L_{3113} = 2\beta\cos^2\alpha,\\
&L_{1332} = L_{2331} = L_{3123} = L_{3132} = L_{3213} = L_{3231} = 2\beta\cos\alpha(\sin\alpha - K\cos\alpha),\\
&L_{2121} = \mu + 2\beta,\\
&L_{2222} = \mu + 2\beta(4\sin^2\alpha - 6K\cos\alpha\sin\alpha + 3K^2\cos^2\alpha),\\
&L_{2323} = \mu + 2\beta\sin^2\alpha,\\
&L_{2332} = L_{3223} = 2\beta(\sin\alpha - K\cos\alpha)^2,\\
&L_{3131} = \mu + 2\beta\cos^2\alpha,\\
&L_{3232} = \mu + 2\beta(\sin\alpha - K\cos\alpha)^2,\\
&L_{3333} = \mu.
\end{aligned}
$$

The symmetric blocks $\mathbf{N}_1$, $\mathbf{N}_2$, and $\mathbf{N}_3$ of the corresponding Stroh matrix $\mathbf{N}$ are given by

$$
-\mathbf{N}_1 = \begin{bmatrix} 0 & 0 & \cos\theta \\ 0 & 0 & \sin\theta \\ \cos\theta & \sin\theta & 0 \end{bmatrix}, \quad \mathbf{N}_2 = \frac{1}{\Delta}\begin{bmatrix} L_{3232} & -L_{1332} & 0 \\ -L_{1332} & L_{3131} & 0 \\ 0 & 0 & 0 \end{bmatrix}, \quad -\mathbf{N}_3 = \begin{bmatrix} \eta & \kappa & 0 \\ \kappa & \nu & 0 \\ 0 & 0 & \chi \end{bmatrix},
$$

respectively, with

$$
\begin{aligned}
&\Delta = L_{3232}L_{3131} - L_{1332}^2 = \mu\left[\mu + 2\beta(1 - 2K\cos\alpha\sin\alpha + K^2\cos^2\alpha)\right],\\
&\eta = (3\mu + L_{1111})\cos^2\theta + 2L_{1121}\cos\theta\sin\theta + L_{2121}\sin^2\theta,\\
&\kappa = L_{1112} + (3\mu + L_{1221})\cos\theta\sin\theta,\\
&\nu = L_{1212}\cos^2\theta + 2L_{1121}\cos\theta\sin\theta + (3\mu + L_{2222})\sin^2\theta,\\
&\chi = \left[\mu\sin 2\alpha + 2\beta(\sin 2\alpha + \sin 2\theta)\right]K + \left[\mu\cos^2\theta + 2\beta(\cos^2\theta - \cos^2\alpha)\right]K^2.
\end{aligned}
$$

Tremendous simplifications occur when L and $\mathbf{N}$ are expressed in the coordinate system aligned with the Lagrangian principal axes and the fibres are aligned with the direction of greatest stretch λ_2. Then, for wrinkles aligned with that direction, we find that

the Stroh matrix reads

$$\mathbf{N} = \begin{bmatrix} 0 & 0 & 0 & \dfrac{\lambda_2^2}{\mu\lambda_2^2 + 2\beta} & 0 & 0 \\ 0 & 0 & -1 & 0 & \dfrac{1}{\mu} & 0 \\ 0 & -1 & 0 & 0 & 0 & 0 \\ -\dfrac{\mu + 2\beta}{\lambda_2^2} & 0 & 0 & 0 & 0 & 0 \\ 0 & -\dfrac{\mu(1 + 3\lambda_2^2)}{\lambda_2^2} & 0 & 0 & 0 & -1 \\ 0 & 0 & \dfrac{\mu(\lambda_2^2 - 1)}{\lambda_2^2} & 0 & -1 & 0 \end{bmatrix}.$$

It clearly shows that the incremental deformation in the plane of shear is uncoupled from the out-of-plane component. Further, the in-plane components do not involve β and are identical to the components of the Stroh matrix for an isotropic neo-Hookean material. It follows that these wrinkles appear at the critical amount of shear $K_{\rm cr} \simeq 3.0873$ found by Destrade et al.[7], independently of the value of β. The corresponding value for the largest stretch is $\lambda_2 = K_{\rm cr}/2 + \sqrt{1 + K_{\rm cr}^2/4} \simeq 3.3830$ and the angle of the fibres in the reference configuration is $\alpha_{\rm cr} = \tan^{-1}(\lambda_2) \simeq 1.283$ rad $= 73.53^\circ$.